

## SUPPORTING INFORMATION

### Ion-exchange resin as a new tool for characterisation of coordination compounds and MOFs by NMR spectroscopy

Ayla Roberta Borges da Silva Galaço,<sup>a</sup> Kleber Thiago de Oliveira,<sup>b</sup> Maria Carolina Donatoni,<sup>b</sup> Richard I. Walton<sup>c</sup> and Osvaldo Antonio Serra<sup>a,d</sup>

<sup>a</sup> University of São Paulo, Chemistry Department, FFCLRP, Ribeirão Preto, Av. Bandeirantes, 3900, 14040-901, Ribeirão Preto – SP, Brazil

<sup>b</sup> Departamento de Química, Universidade Federal de São Carlos, São Carlos, SP, 13565-905, Brazil.

<sup>c</sup> University of Warwick, Department of Chemistry, Coventry CV4 7AL, U.K

<sup>d</sup> Universidade Federal do ABC, CCNH, Av. dos Estados, 5001, 09210-580, Santo André – SP, Brasil

#### **S1: General Methods**

The starting materials and solvents were obtained from the commercial supplier Aldrich and used without further purification. <sup>1</sup>H NMR and <sup>13</sup>C NMR spectra were recorded on BRUKER(R) DRX400 Ultra Shield (R) spectrometers (400 MHz and 500 MHz). Thermogravimetric analysis (TGA) was performed at a scan speed of 10°C/min under air on TA Instrument Q600 SDT.

#### **S2: Experimental Details for HKUST-1 [Cu<sub>2</sub>(btc)<sub>3</sub>] preparation.<sup>1</sup>**

Benzene-1,3,5-tricarboxylic acid – H<sub>3</sub>btc (10 mmol) and copper(II) nitrate hemipentahydrate (10 mmol) were stirred for 15 min in 50 mL of solvent consisting of equal parts of *N,N*-dimethylformamide (DMF), ethanol and deionized water in a 250 mL volume Teflon autoclave. The solution was heated at 180°C for 12 h to yield a blue, polycrystalline powdered sample of the desired phase. The recovered solid material was washed with DMF at room temperature for purification.

#### **S3: Experimental details for [[Eu<sub>2</sub>(H<sub>2</sub>O)<sub>5</sub>(ptc)<sub>2</sub>]·H<sub>2</sub>O] preparation.**

A synthesis method reported in the literature was followed.<sup>2</sup> A mixture of pyridine-2,4,6-tricarboxylic acid (H<sub>3</sub>ptc) (0.2 mmol), EuCl<sub>3</sub>·6H<sub>2</sub>O (0.2 mmol, 4.15 mL (0.04824 mol/L)) and H<sub>2</sub>O (15 mL) was placed in a 25 mL Teflon-lined autoclave, which was heated to 180 °C for 72 h. The recovered solid material was washed with water at room temperature.

#### **S4: Experimental Details for [Gd<sub>2</sub>(ofd)<sub>3</sub>·8H<sub>2</sub>O] preparation.**<sup>3</sup>

The compound was prepared by the slow addition of *o*-phenylenedioxydiacetic acid (1.5 mmol) to the GdCl<sub>3</sub> solution (1 mmol). The pH of the obtained mixture was adjusted to 6.04, and this was heated at 65 °C, thus obtained a precipitate. The precipitate was filtered off and dried under vacuum.

#### **S5: Experimental Details for IRMOF-3 preparation.**<sup>4</sup>

Zn(NO<sub>3</sub>)<sub>2</sub>·6H<sub>2</sub>O (6 mmol) and 2-aminoterephthalic acid (2 mmol) were dissolved in *N,N*-dimethylformamide (DMF 50 mL) at room temperature. The obtained solution was sealed and placed in the oven at 100°C for 18 h. The obtained crystals were washed with DMF (five times), chloroform (five times), then immersed into chloroform overnight to remove DMF guest molecules from IRMOF-3.

#### **S6: Experimental Details for Functionalization of IRMOF-3 with ethyl isocyanate.**<sup>5</sup>

30 mg dried IRMOF-3 crystals (0.15 mmol equiv of –NH<sub>2</sub>) were suspended in 1.00 mL chloroform (CHCl<sub>3</sub>) and 60 μL (0.75 mmol) ethyl isocyanate was then added to the mixture. The vial was capped and left on the bench for a period of 12 hours. The reaction was stopped by removing the reaction solution and washing the solids 10 times with CHCl<sub>3</sub>. The solids were suspended in 10 mL of CHCl<sub>3</sub> and kept for 24 h. After, the solid was dried under vacuum for 24 h and the modified product (IRMOF-3-EISC) was obtained.

#### **S7: Experimental Details for Modification of IRMOF-3 with benzyl bromide.**

To an ACE® pressure tube was added the IRMOF-3 (100 mg, 0,122 mmol), dry tetrahydrofuran (2 mL) and then benzyl bromide (52,0 μL, 0,438 mmol). The resulting mixture was kept under magnetic stirring for 72 h and then the reaction was filtered off. The resulting precipitated was washed with saturated sodium bicarbonate aqueous solution (3 x 10 mL), distilled water (3 x 10 mL) and then with tetrahydrofuran (3 x 10 mL). The isolated solid was dried under vacuum at 60 °C and then characterized by <sup>1</sup>H and <sup>13</sup>C NMR.

#### **S8: Experimental details for MIL-53 Fe(OH)<sub>0.8</sub>F<sub>0.2</sub>[bdc] preparation.**<sup>6</sup>

Fluorinated MIL-53(Fe) was synthesised from a mixture of iron(III) chloride hexahydrate (FeCl<sub>3</sub>·6H<sub>2</sub>O), benzene-1,4-dicarboxylic acid (HO<sub>2</sub>C-(C<sub>6</sub>H<sub>4</sub>)-CO<sub>2</sub>H), hydrofluoric acid (HF, 40% in water), *N,N*-dimethylformamide (HCON(CH<sub>3</sub>)<sub>2</sub>) and deionised water in the molar ratio 1:1:65:1:8. Reactants were added to a Teflon liner (~15-20 ml in volume) and the solution was stirred by 5 minutes using a magnetic stirring bar. The Teflon liner was sealed inside a stainless-steel autoclave, which was subsequently placed in a thermostatically-controlled fan oven. The standard heating programme involved heating from room temperature to 150 °C with a ramp rate of 10 °C per minute keeping at 150 °C during 12h. After that, the cooling to room

temperature was performed with a ramp rate of 50 °C per minute. The final product was filtered off, washed twice with methanol and dried under air for one hour, giving a yellow pale powder.

### S9: Thermogravimetric Analysis

#### S9.1 HKUST-1

Prior to analysis the sample was dried in vacuum at 100 °C to remove any excess solvent; the sample then exposed to air contains only water. A first mass loss is due to crystal water, both directly coordinated and trapped within the porous structure, followed by an abrupt mass loss due to the combustion of the ligand at ~300 °C. This is consistent with the literature, where similar TGA profiles have been presented.<sup>7</sup>

Chemical composition	Temperature	% Mass Measured	% Mass Expected
$\text{Cu}_3(\text{btc})_2(\text{H}_2\text{O})_3 \cdot 5.4\text{H}_2\text{O}$	25 °C	100.0	100.0
$\text{Cu}_3(\text{btc})_2$	312 °C	80.00	80.00
3Cu	600 °C	26.10	25.20

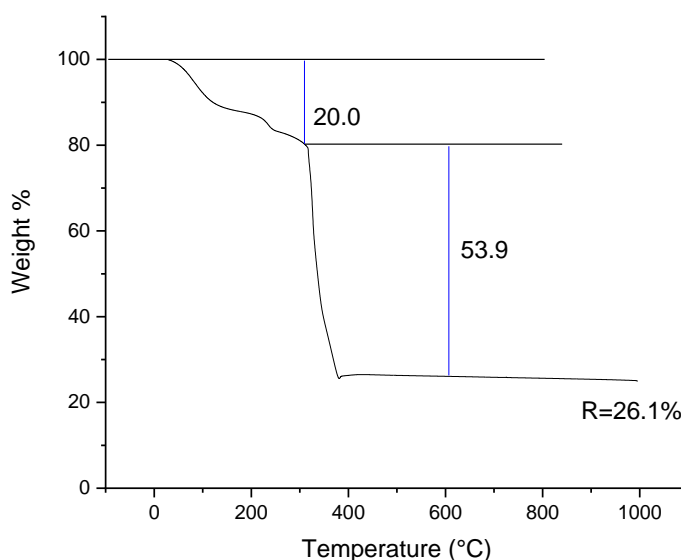


**Figure S1: Thermogravimetric analysis of HKUST-1**

#### S9.2 $[\text{Eu}_2(\text{H}_2\text{O})_5(\text{ptc})_2] \cdot \text{H}_2\text{O}$

The TGA shows a mass loss up to 200 °C due to loss of water of coordination and hydration, followed by combustion of the organic ligand to finally produce  $\text{Eu}_2\text{O}_3$  above 800 °C. The results are similar to reported by Lin *et al.* for the isostructural dysprosium material.<sup>8</sup>

Chemical composition	Temperature	% Mass Measured	% Mass Expected
$[\text{Eu}_2(\text{ptc})_2 \cdot 6\text{H}_2\text{O}]$	25 °C	100.0	100.0
$\text{Eu}_2(\text{ptc})_2$	200 °C	86.38	86.96
$\text{Eu}_2\text{O}_3$	800 °C	42.88	44.40

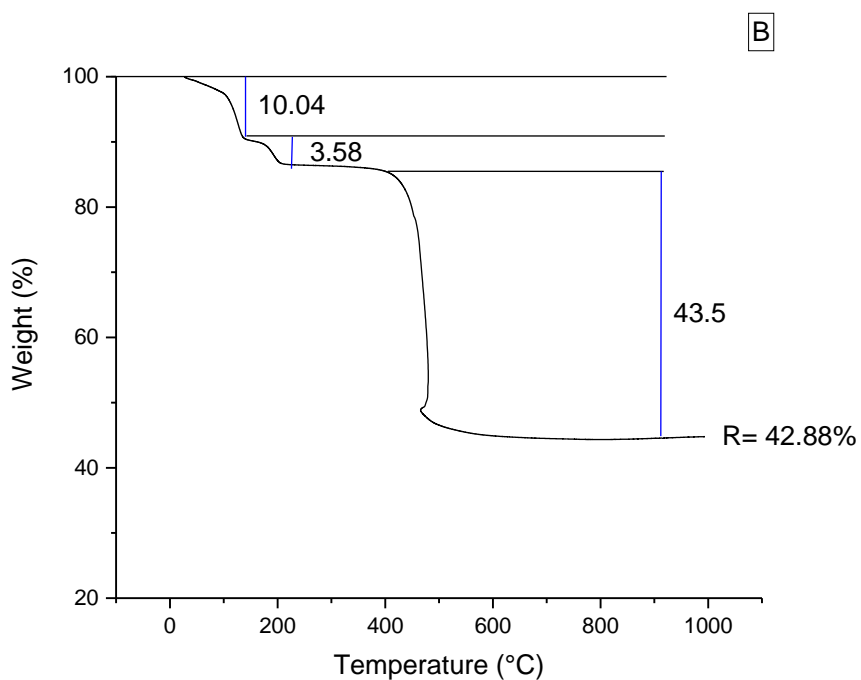


**Figure S2: Thermogravimetric analysis of  $[\text{Eu}_2(\text{H}_2\text{O})_3(\text{ptc})_2] \cdot \text{H}_2\text{O}$**

### **S9.3 $[\text{Gd}_2(\text{ofd})_3 \cdot 8\text{H}_2\text{O}]$**

The TGA shows a mass loss up to 150 °C due to loss of water of coordination, followed by combustion of the organic ligand to finally produce  $\text{Gd}_2\text{O}_3$  above 800 °C. The results are similar to reported by Jiang.<sup>3</sup>

<b>Chemical composition</b>	<b>Temperature</b>	<b>% Mass Measured</b>	<b>% Mass Expected</b>
$[\text{Gd}_2(\text{ofd})_3 \cdot 8\text{H}_2\text{O}]$	25 °C	100.0	100.0
$\text{Gd}_2(\text{ofd})_3$	150° C	89.17	87.33
$\text{Gd}_2\text{O}_3$	800°C	32.37	31.87

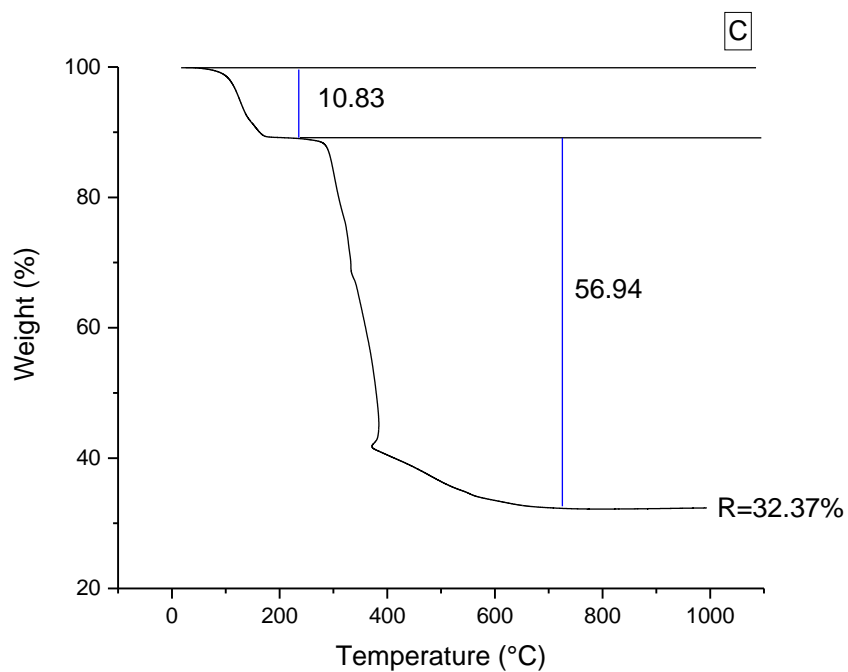


**Figure S3: Thermogravimetric analysis of  $[Gd_2(ofd)_3 \cdot 8H_2O]$**

#### **S9.4 IRMOF-3**

The TGA shows a mass loss up to 600 °C due the combustion of the organic ligand to produce ZnO. The results are similar to reported by Cohen <sup>5</sup>

<b>Chemical composition</b>	<b>Temperature</b>	<b>% Mass Measured</b>	<b>% Mass Expected</b>
Zn <sub>4</sub> O(H <sub>2</sub> N-bdc) <sub>3</sub>	25 °C	100.0	100.0
ZnO	600°C	36.88	37.99

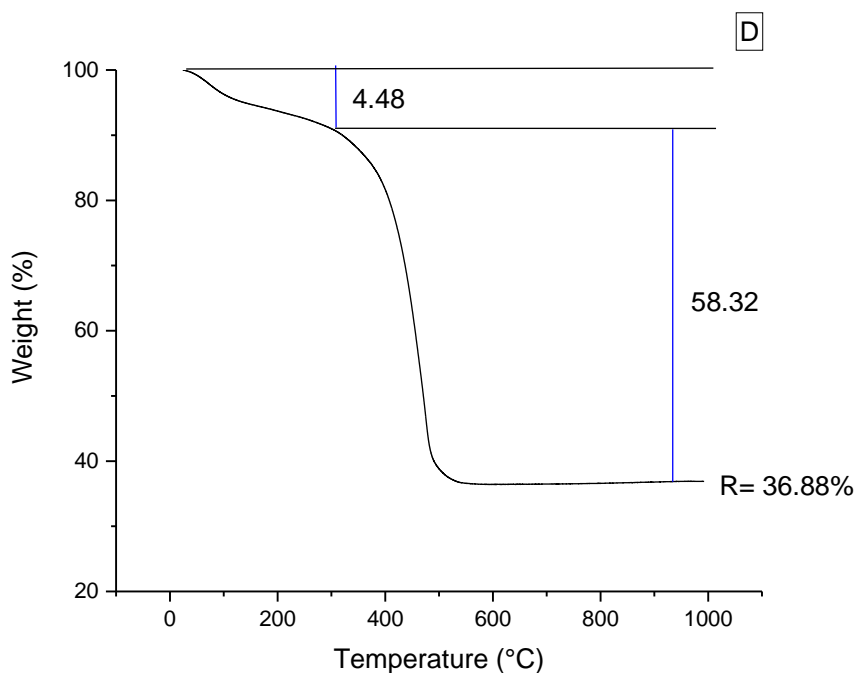


**Figure S4: Thermogravimetric analysis of IRMOF-3**

### **S9.5 IRMOF-3-isocyanate**

The TGA shows a mass loss up to 250 °C due to loss of ethyl isocyanate, followed by combustion of the organic ligand, 2-amino-1,4-benzene dicarboxylic acid, to finally produce ZnO above 600 °C. This is consistent with the literature.<sup>5</sup>

Chemical composition	Temperature	% Mass Measured	% Mass Expected*
[ZnO <sub>1/4</sub> (C <sub>3</sub> H <sub>6</sub> ON-NH-C <sub>8</sub> H <sub>4</sub> O <sub>4</sub> ) <sub>3/4</sub> ]	25 °C	100.0	100.0
[ZnO <sub>1/4</sub> (NH-C <sub>8</sub> H <sub>4</sub> O <sub>4</sub> ) <sub>3/4</sub> ]	250 °C	74.82	72.26
ZnO	600 °C	36.00	31.64

\* considering 100% of modification.

#### **TGA based calculation of IRMOF-3.pre-modified and post-synthetic modification.**

IRMOF-3 [ZnO<sub>1/4</sub>(C<sub>8</sub>H<sub>3</sub>O<sub>4</sub>-NH<sub>2</sub>)<sub>3/4</sub>]; Calculated MW: 203 g/mol

Residue: 37.0% (ZnO), Experimental MW: 219 g/mol

IRMOF-3-ethyl isocyanate [ZnO<sub>1/4</sub>(C<sub>3</sub>H<sub>6</sub>ON-NH-C<sub>8</sub>H<sub>3</sub>O<sub>4</sub>)<sub>3/4</sub>] Calculated MW: 256 g/mol

#### **Post modified IRMOF-3 with ethyl isocyanate**

Residue: 35.9% (ZnO), Experimental MW: 225 g/mol

Experimental MW difference between IRMOF-3 and IRMOF-3-ethyl isocyanate

225 – 219 = 6 MW units; if 100% was modified the difference will be 256 – 203 = 53

So, the percentage of modification is  $6 \times \frac{100}{53} = 11.3\%$

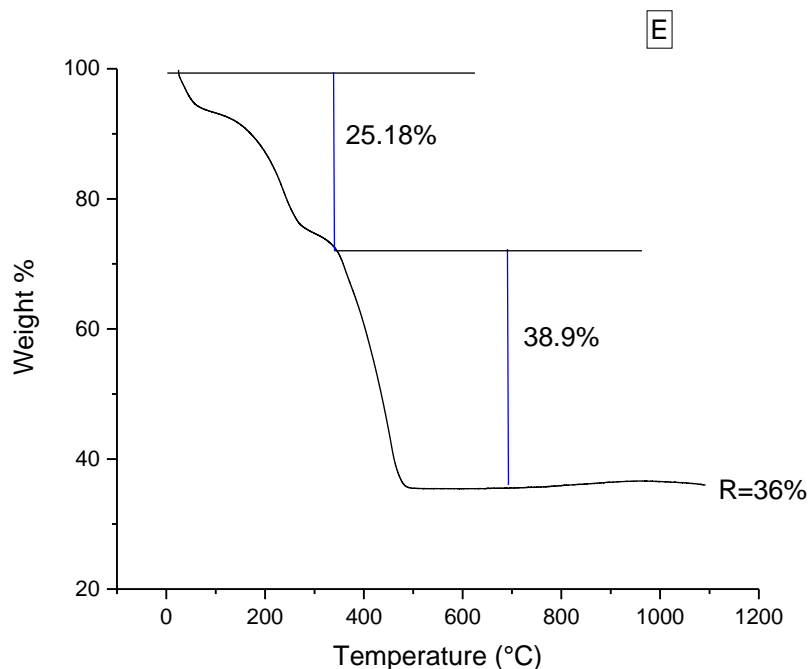


**Figure S5: Thermogravimetric analysis of IRMOF-3-isocyanate**

### **S9.6 IRMOF-3-benzyl bromide**

The TGA shows a mass loss up to 300 °C due to loss of the benzyl functionalisation, followed by combustion of the organic ligand, 2-amino-1,4-benzene dicarboxylic acid, to finally produce ZnO above 800 °C.

<b>Chemical composition</b>	<b>Temperature</b>	<b>% Mass Measured</b>	<b>% Mass Expected*</b>
[ZnO <sub>1/4</sub> (C <sub>8</sub> H <sub>4</sub> O <sub>4</sub> -NH-CH <sub>2</sub> -C <sub>6</sub> H <sub>5</sub> ) <sub>3/4</sub> ]	25 °C	100.0	100.0
[ZnO <sub>1/4</sub> (NH-C <sub>8</sub> H <sub>4</sub> O <sub>4</sub> ) <sub>3/4</sub> ]	300 °C	89.70	66.42
ZnO	800°C	34.40	29.89

\* considering 100% of modification.

### **TGA based calculation of IRMOF-3.pre-modified and post-synthetic modification.**

IRMOF-3 [ZnO<sub>1/4</sub>(C<sub>8</sub>H<sub>3</sub>O<sub>4</sub>-NH<sub>2</sub>)<sub>3/4</sub>]; Calculated MW: 203 g/mol

Residue: 37.0% (ZnO), Experimental MW: 219 g/mol

IRMOF-3-benzyl bromide [ZnO<sub>1/4</sub>(C<sub>3</sub>H<sub>6</sub>ON-NH-CH<sub>2</sub>-C<sub>6</sub>H<sub>5</sub>)<sub>3/4</sub>] Calculated MW: 271 g/mol

### Post modified IRMOF-3 with benzyl bromide

Residue: 34.4% (ZnO), Experimental MW: 235.5 g/mol

Experimental MW difference between IRMOF-3 and IRMOF-3-benzyl bromide

$235.5 - 219 = 16.5$  MW units; if 100% was modified the difference will be  $271 - 203 = 68$

So, the percentage of modification is  $16.5 \times \frac{100}{68} = 24\%$

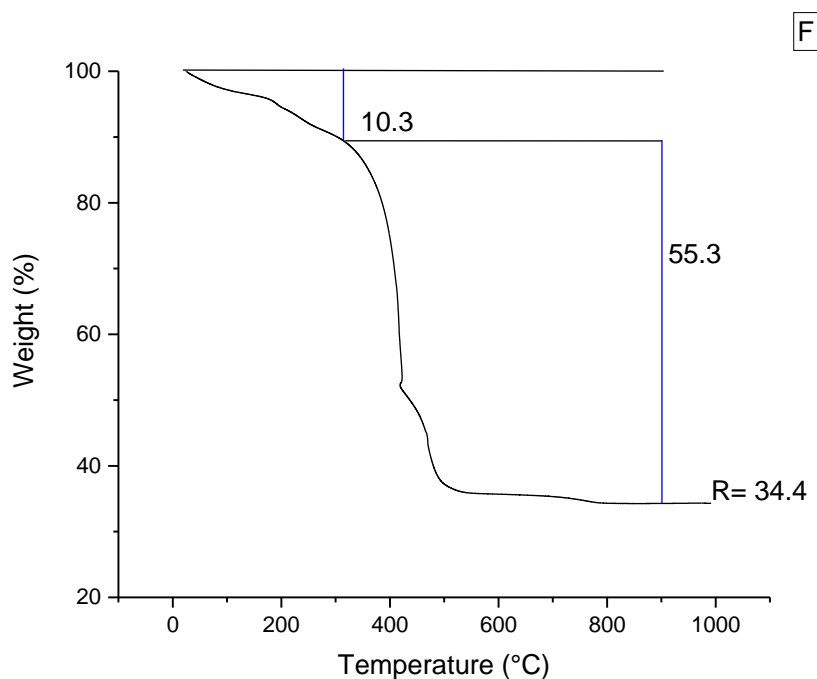


**Figure S6: Thermogravimetric analysis of IRMOF-3-benzyl bromide**

### S9.7 MIL-53(Fe)

The TGA shows a mass loss up to 250 °C due to loss of water of hydration, followed by combustion of the organic ligand to finally produce Fe<sub>2</sub>O<sub>3</sub> above 400 °C. The results are similar to reported by Millange *et al.*<sup>6</sup>

Chemical composition	Temperature	% Mass Measured	% Mass Expected
Fe(OH) <sub>0.8</sub> Fo.2[bdc]·1.5H <sub>2</sub> O	25 °C	100.0	100.0
Fe(OH) <sub>0.8</sub> Fo.2[bdc]	250 °C	88.84	89.77
½ Fe <sub>2</sub> O <sub>3</sub>	600 °C	30.81	30.30



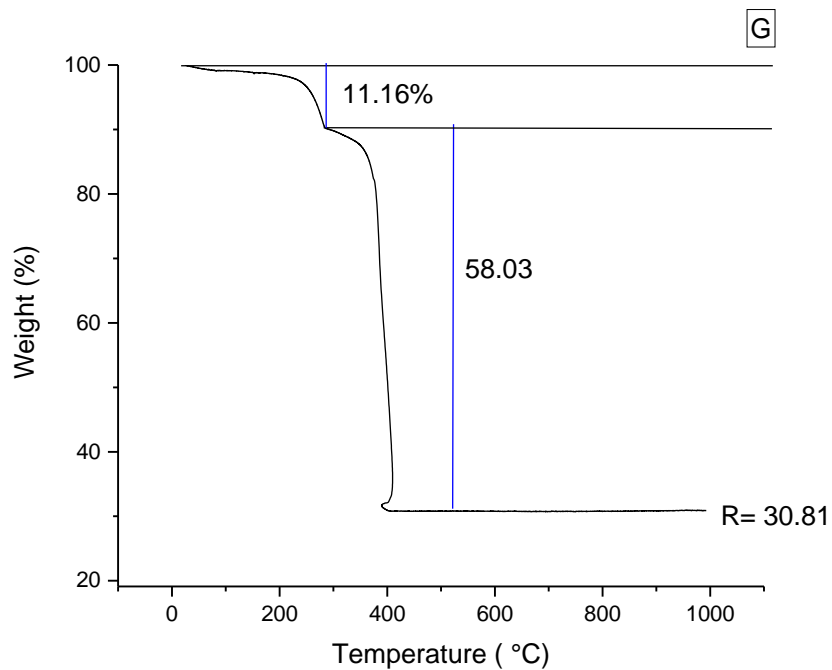


**Figure S7: Thermogravimetric analysis of MIL-53(Fe)**

**S10: Powder X-ray diffraction.**

Powder XRD patterns were recorded using Cu  $K\alpha_{1/2}$  radiation from powdered samples in reflection geometry. The measured patterns are compared with simulated patterns using the published crystal structures of the materials. Note that in some cases, preferred orientation effects in the reflection geometry lead to different relative peak intensities in the measured patterns.

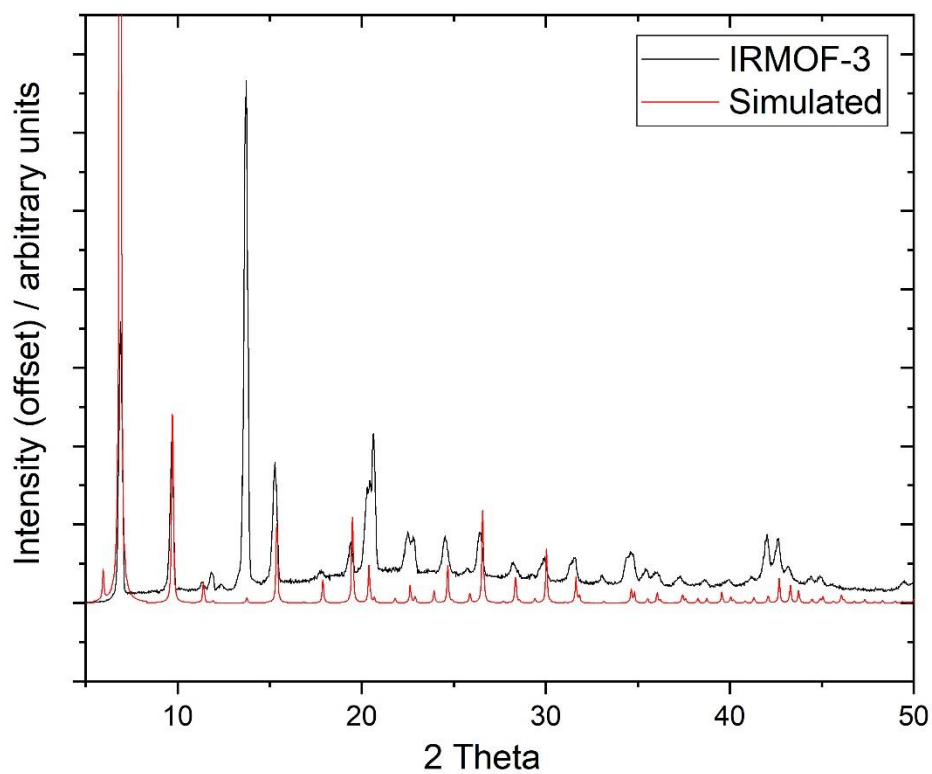


**Figure S8: Powder XRD of IRMOF-3**

The powder XRD pattern for IRMOF-3 is typical of patterns reported in the literature for samples of the same material, which also effects of preferred orientation, solvent content and particle size of the relative intensities of Bragg peaks recorded, see, for example refs 9-11.

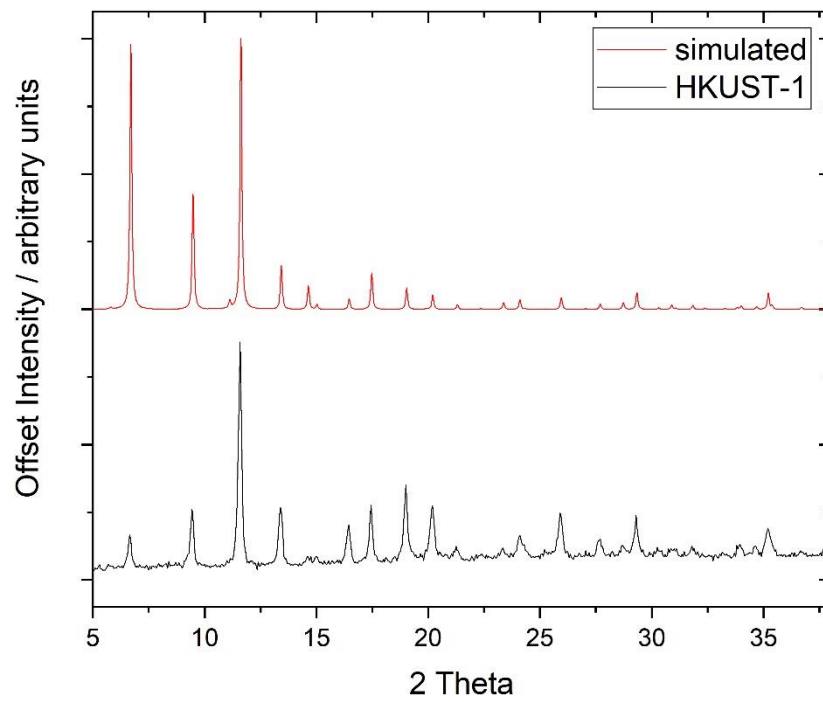


**Figure S9: Powder XRD of HKUST-1**

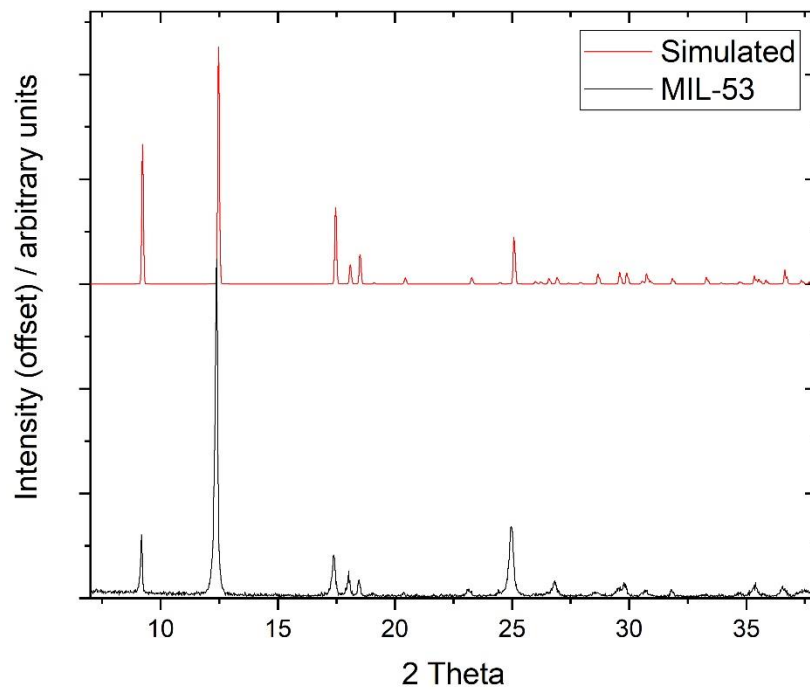


**Figure S10: Powder XRD of MIL-53(Fe)**

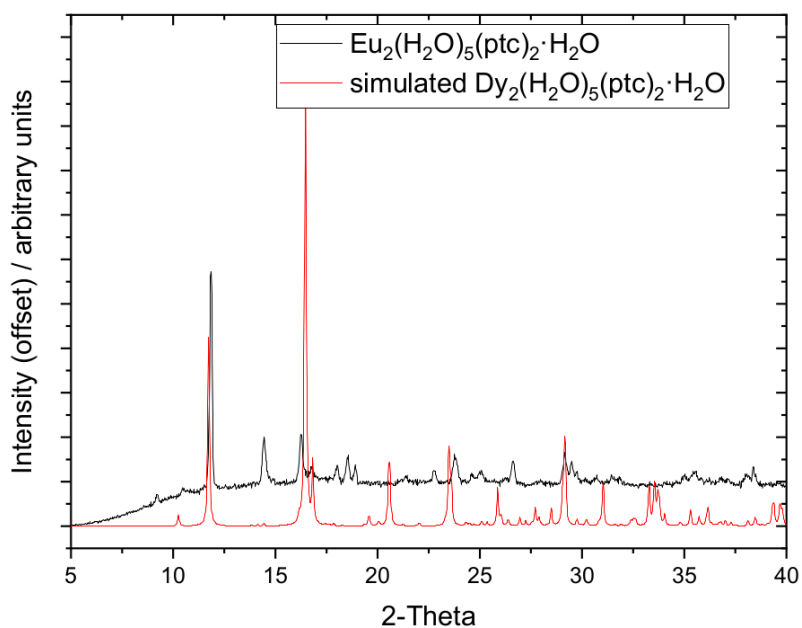


**Figure S11: Powder XRD of  $[\text{Eu}_2(\text{H}_2\text{O})_5(\text{ptc})_2] \cdot \text{H}_2\text{O}$ . The simulated pattern is that of the isostructural  $[\text{Dy}_2(\text{H}_2\text{O})_5(\text{ptc})_2] \cdot \text{H}_2\text{O}$  reported by Lin *et al.*<sup>8</sup> Note the effects of preferred orientation and the shift in Bragg peaks due to the variation of lattice parameters.**

The powder XRD of  $[\text{Eu}_2(\text{H}_2\text{O})_5(\text{ptc})_2] \cdot \text{H}_2\text{O}$  may also indicate the presence of at least one impurity. However, this is not unreacted pyridine-tricarboxylic acid and it does not match any of the lanthanide pyridine-tricarboxylates reported on the CSD. Since the thermogravimetric analysis is in very good agreement with the bulk composition (see above) the impurity phase(s) must be present in small amounts, or are polymorphs of the major phase.

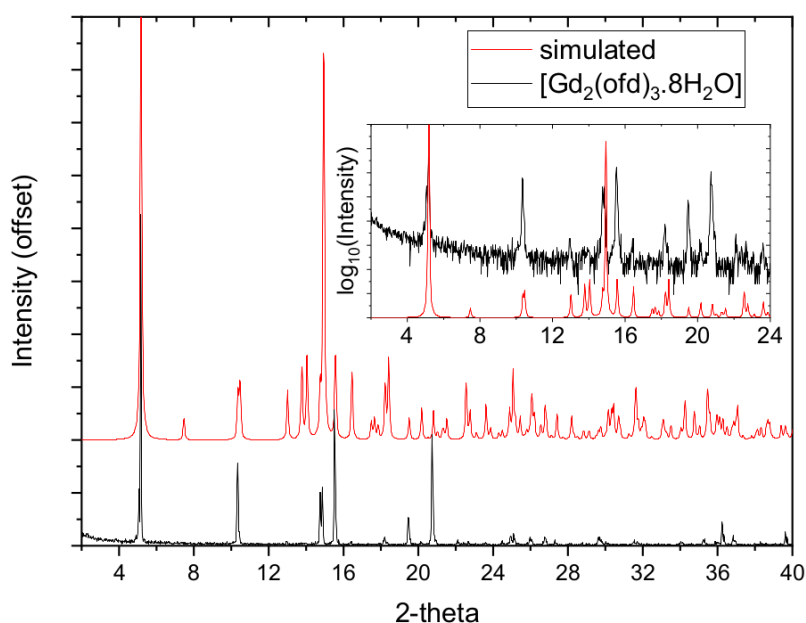


**Figure S12: Powder XRD of  $[\text{Gd}_2(\text{ofd})_3 \cdot 8\text{H}_2\text{O}]$ . The inset is a plot with a logarithmic intensity scale to show the weak diffraction peaks obscured by severe preferred orientation.**

## S11: NMR

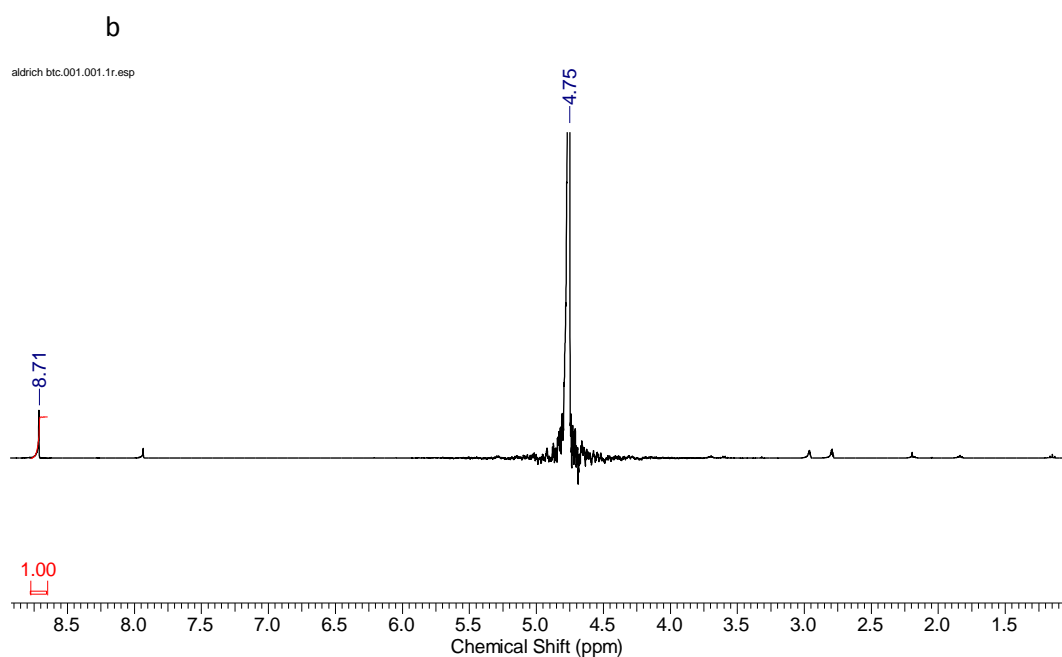
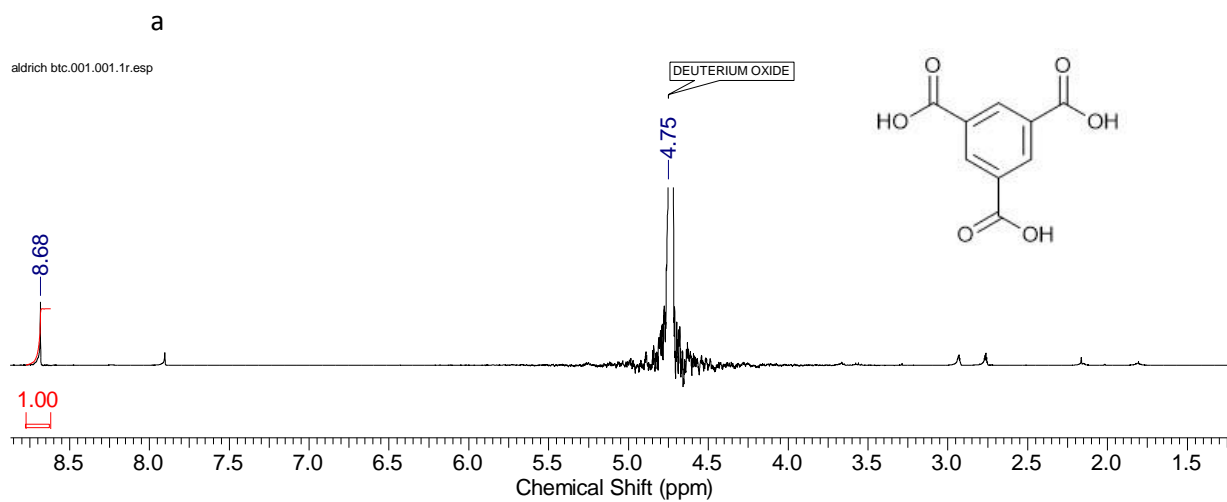
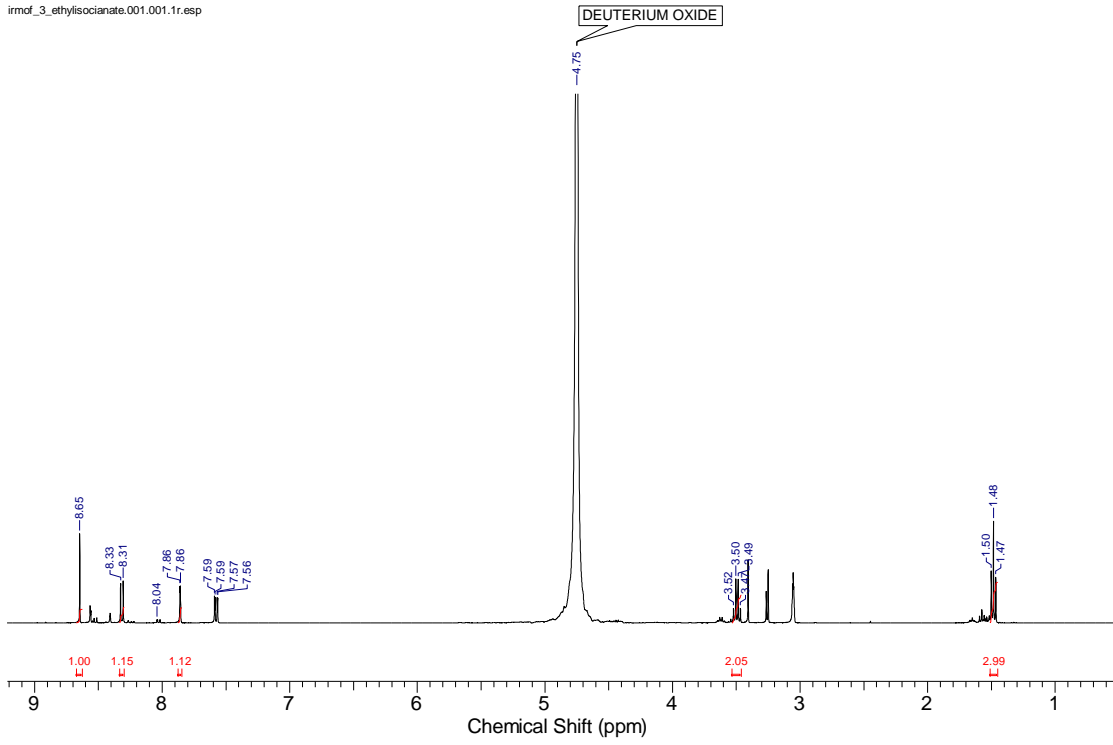


Figure S13:  $^1\text{H}$  NMR of trimesic acid from (a) MOF HKUST-1 after treatment with the resin and (b) commercial standard obtained from Aldrich and analysed in the same deuterated solvent mixture CAS 554-95-0

a)

irmof\_3\_ethylisocyanate.001.001.1r.esp



b)

irmof\_3\_ethylisocyanate.015.001.1r.esp

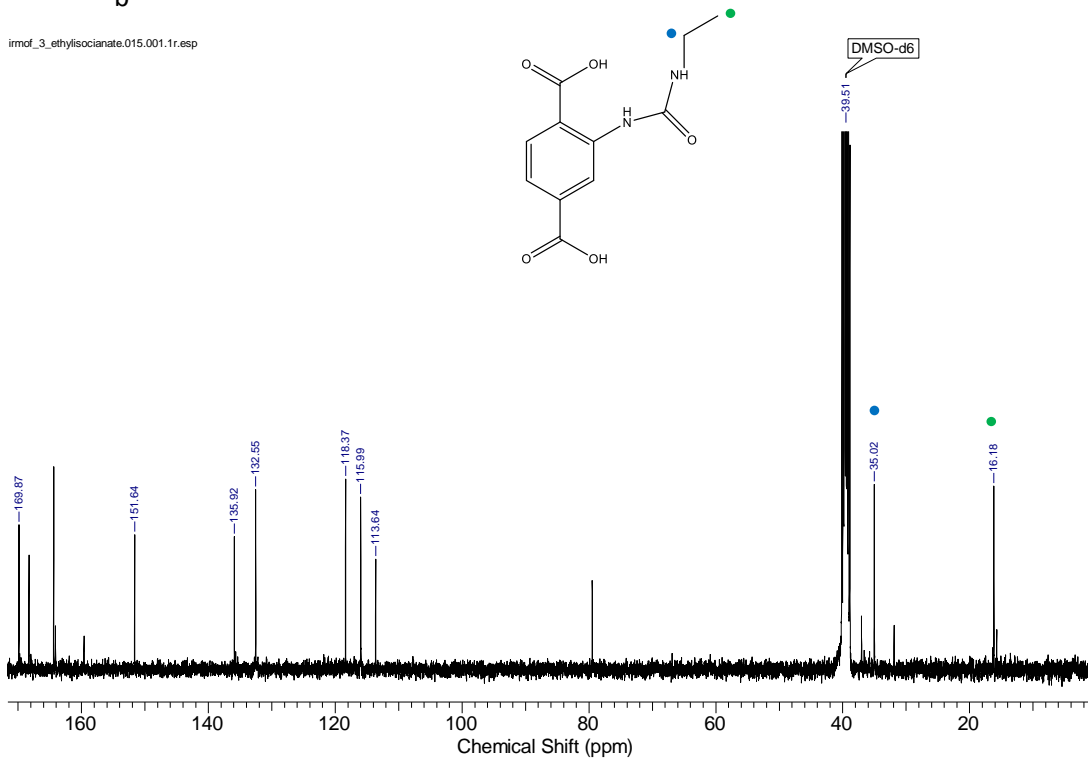
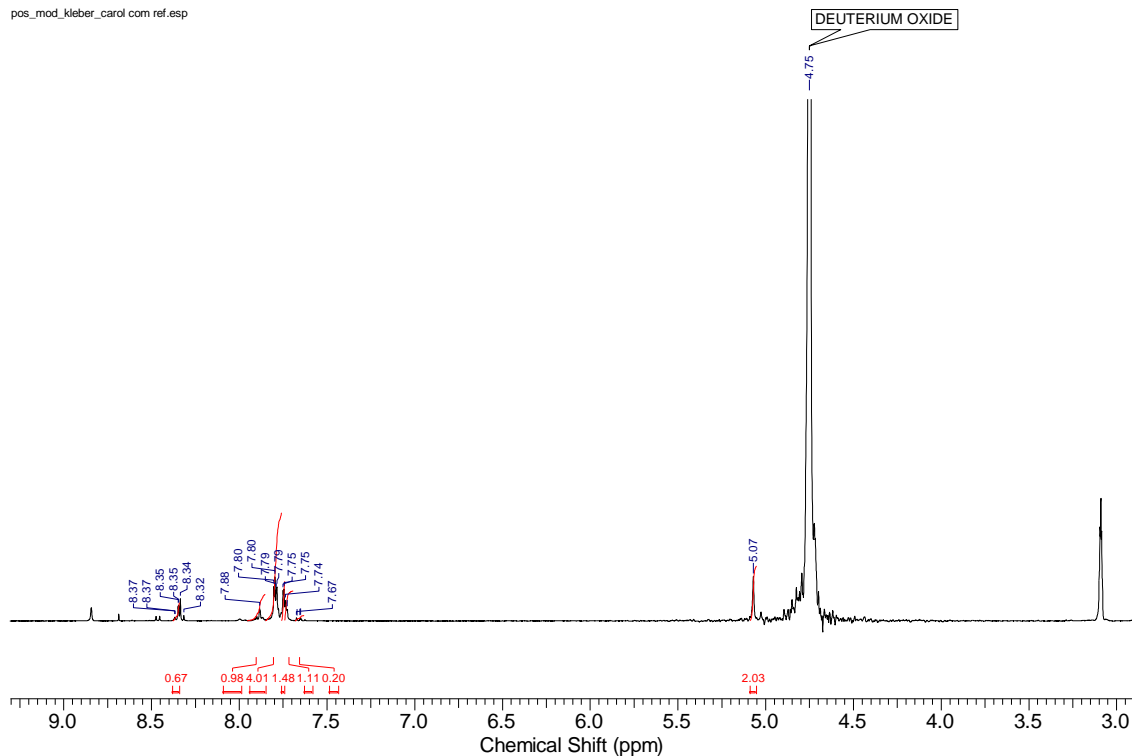


Figure S14: (a)  $^1\text{H}$  NMR and (b)  $^{13}\text{C}$  NMR of the MOF IRMOF-3 post modified with ethyl isocyanate (IRMOF-3-EISCN).

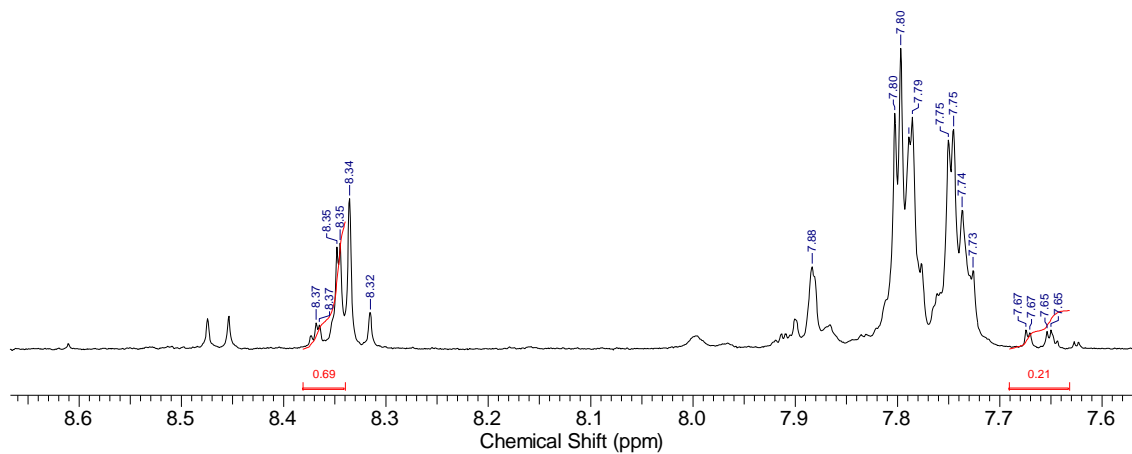
a

pos\_mod\_kleber\_carol.com.ref.esp



pos\_mod\_kleber\_carol.com.ref.esp

b



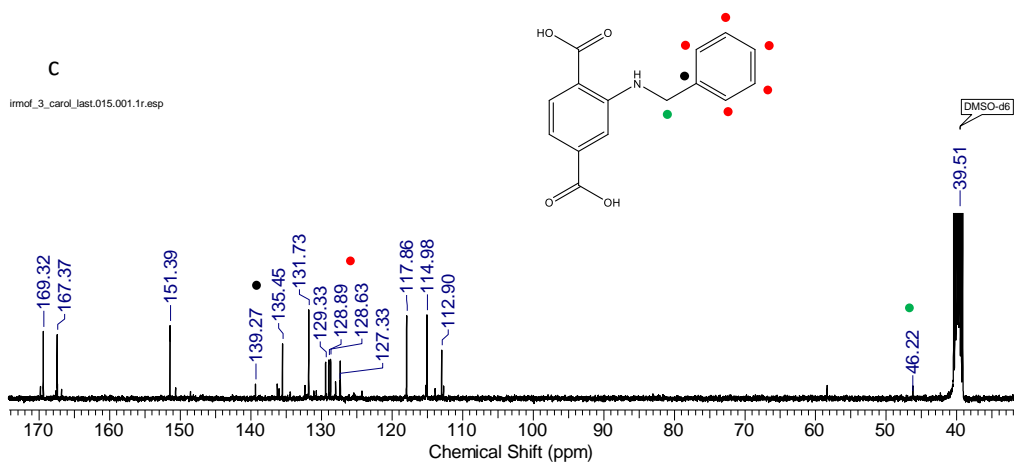
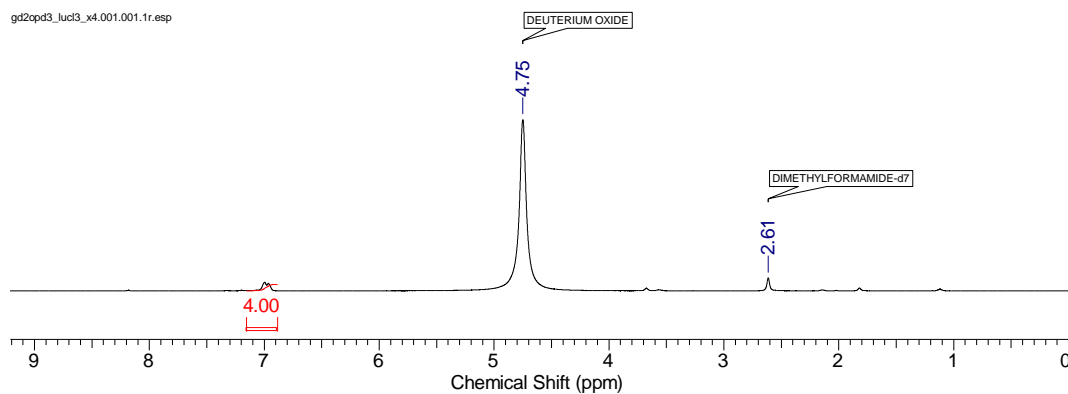


Figure S15:(a)  $^1\text{H}$  NMR (b)  $^1\text{H}$  NMR quantitative determination of post-functionalisation, and (c)  $^{13}\text{C}$  NMR of the MOF IRMOF-3 post modified with benzyl bromide.

a)



b)

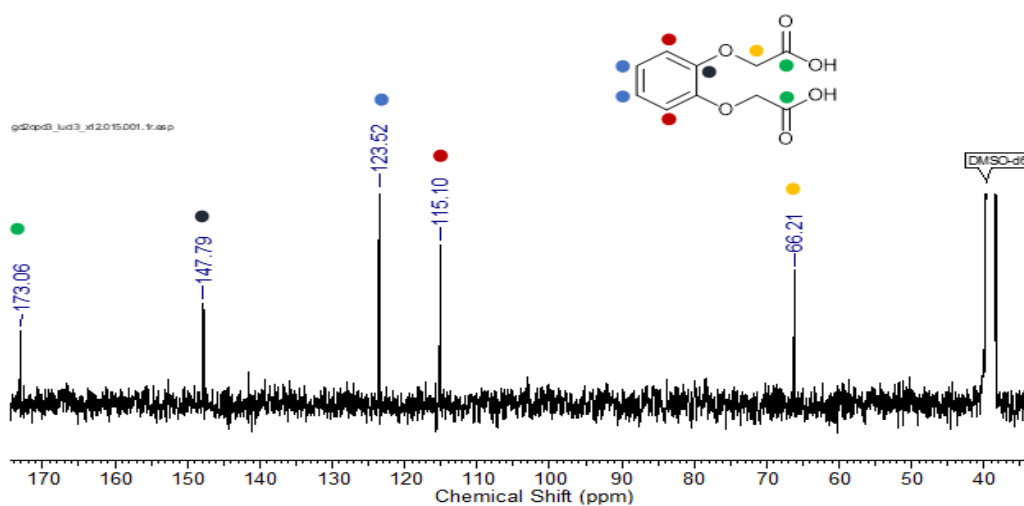


Figure S16: (a)  $^1\text{H}$  NMR (b)  $^{13}\text{C}$  NMR of o-phenylenedioxydiacetate from the  $[\text{Gd}_2(\text{ofd})_3 \cdot 8\text{H}_2\text{O}]$  complex



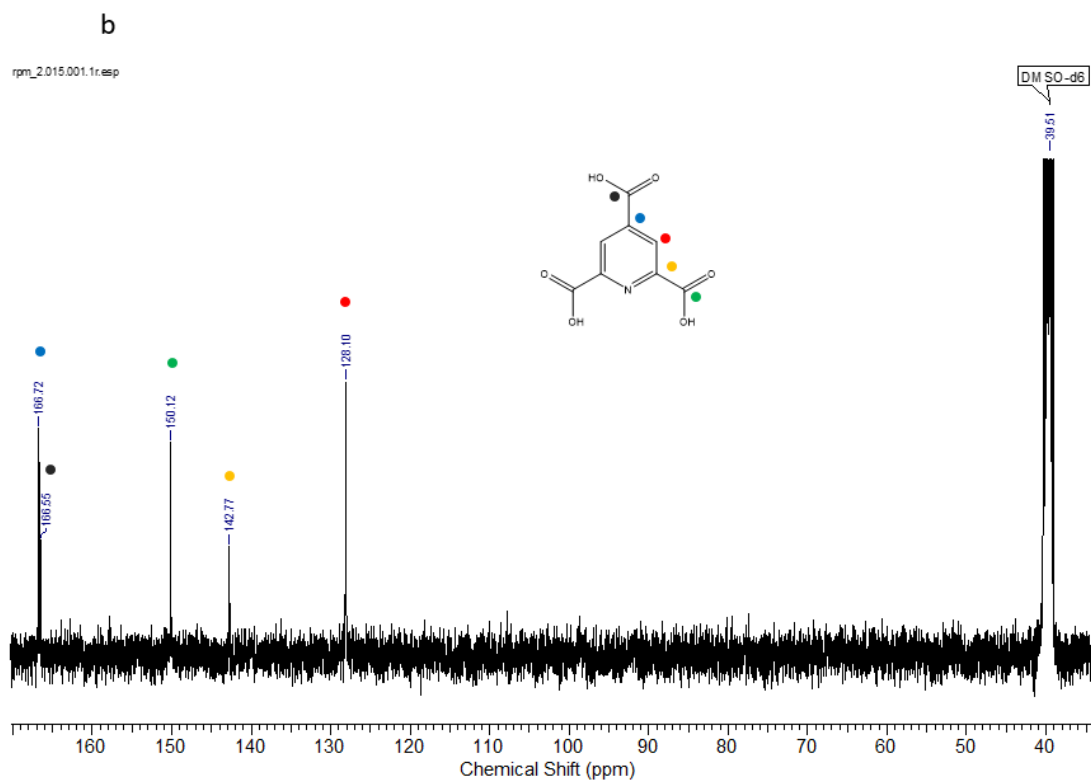
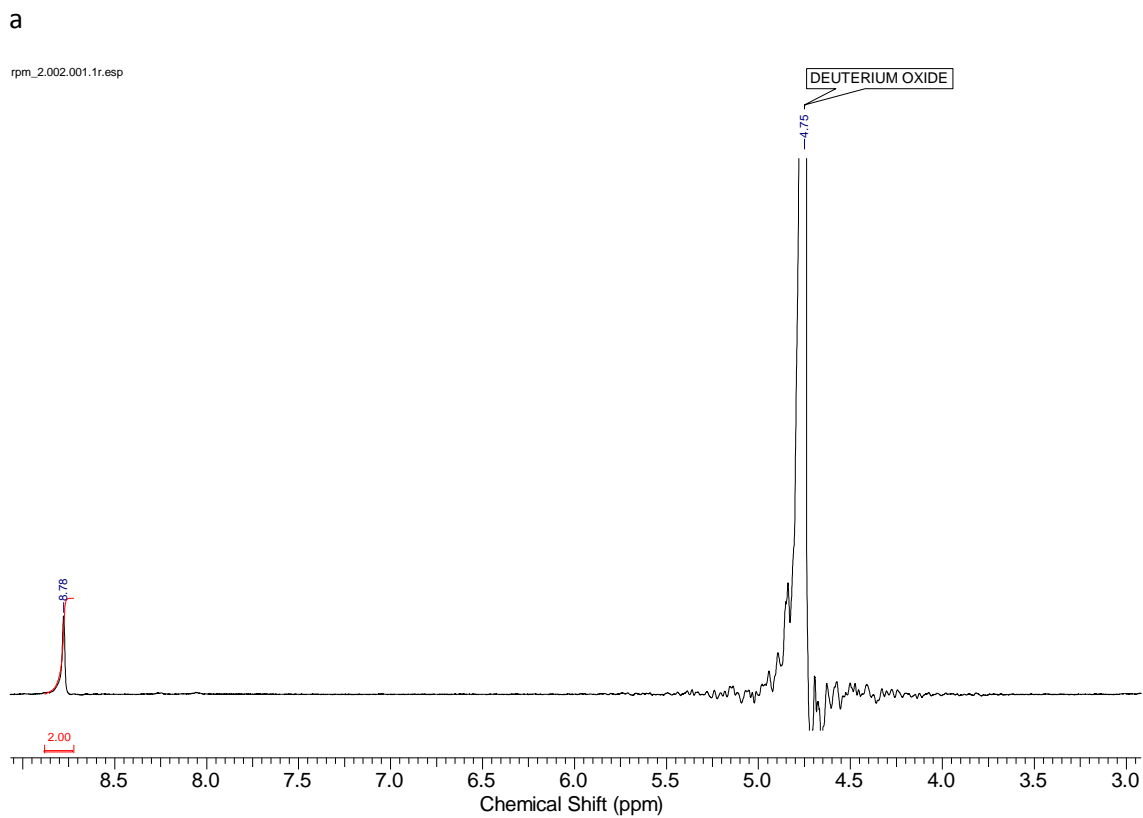
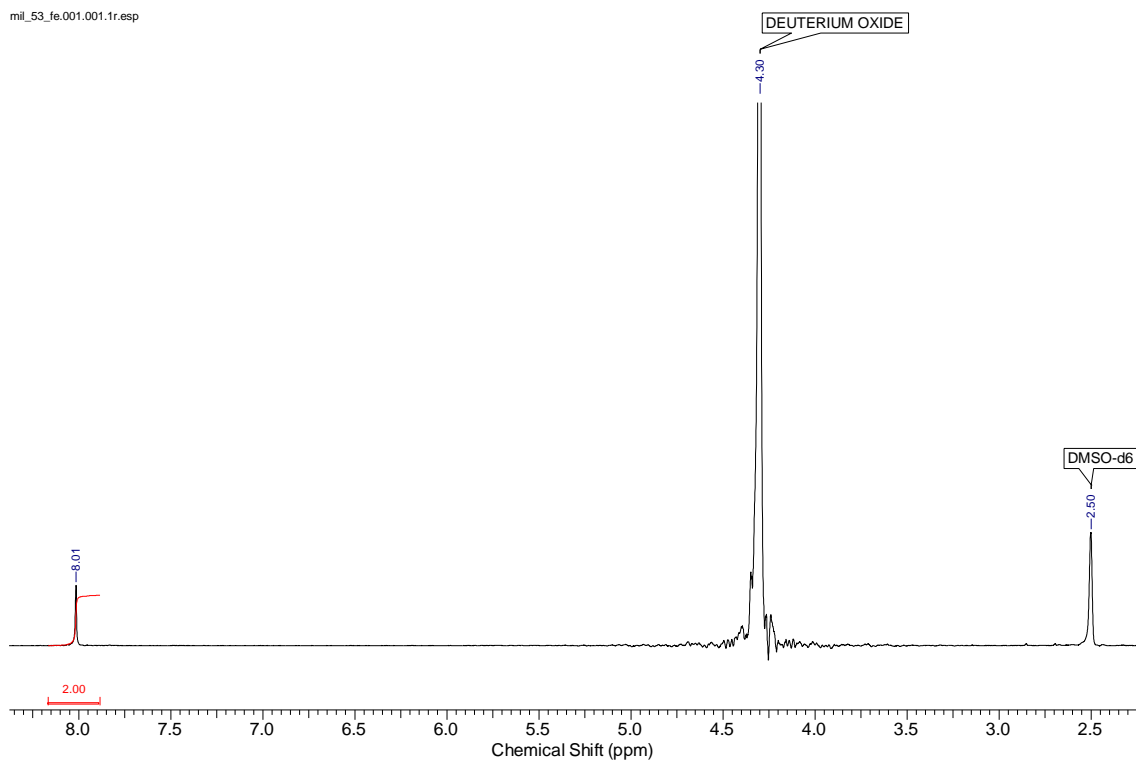


Figure S17: (a)  $^1\text{H}$  NMR; (b)  $^{13}\text{C}$  NMR of pyridine tricarboxylic acid from the compound  $[\text{Eu}_2(\text{H}_2\text{O})_5(\text{ptc})_2]\cdot\text{H}_2\text{O}$ .

a)

mil\_53\_fe.001.001.1r.esp



b)

mil\_53\_fe.015.001.1r.esp

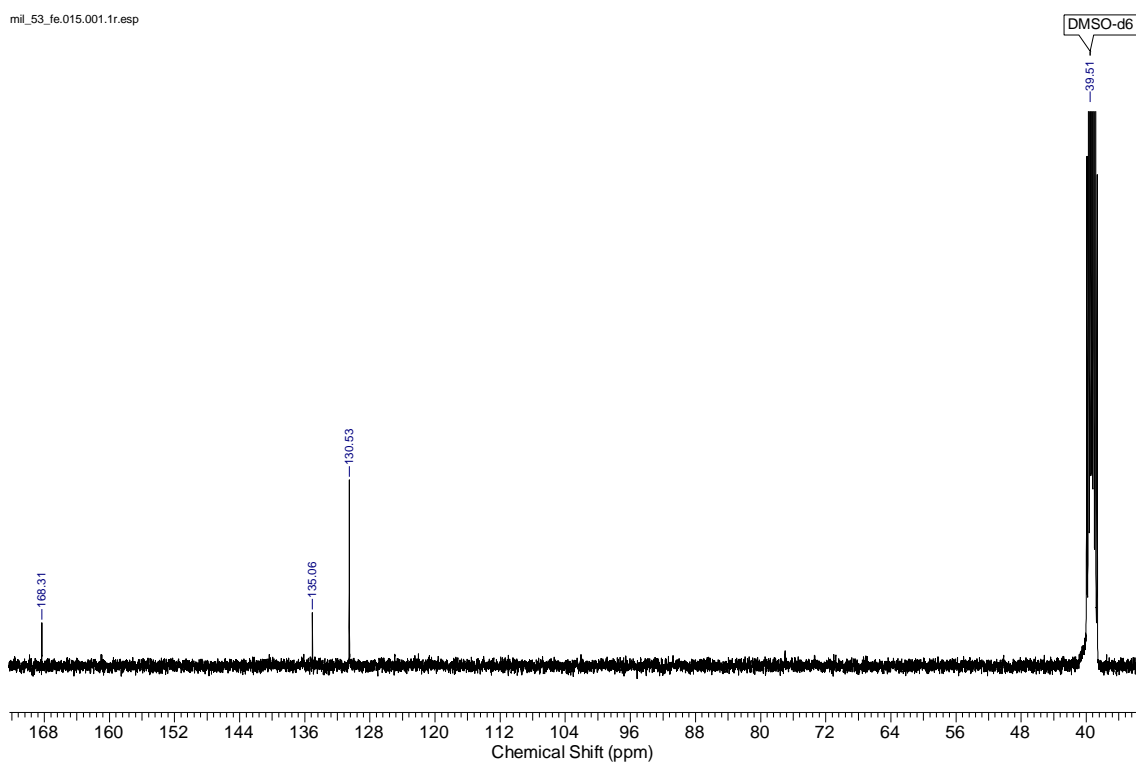
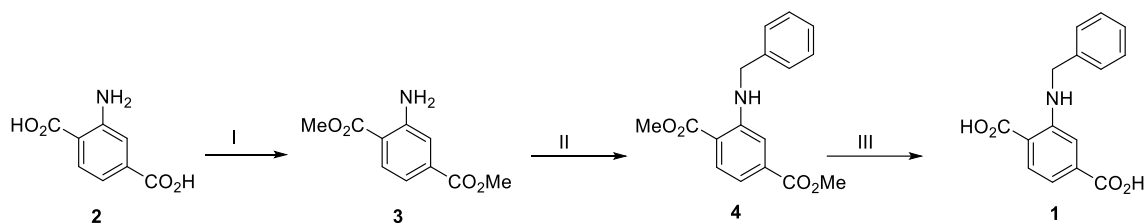


Figure S18: (a)  $^1\text{H}$  NMR (b)  $^{13}\text{C}$  NMR of MIL-53 MIL-53  $\text{Fe}(\text{OH})_{0.8}\text{F}_{0.2}[\text{bdc}]$ .

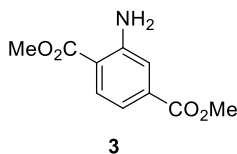
### S12: Synthesis of 2-benzylaminoterephthalic acid (1)

The 2-benzylaminoterephthalic acid (**1**) was synthesized from 2-aminoterephthalic acid following the steps showed in Scheme below:



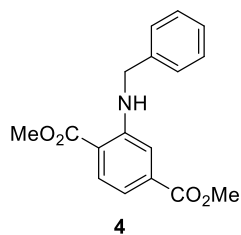
Scheme S1: I) H<sub>2</sub>SO<sub>4</sub>, MeOH, 18 h, reflux. II) Benzyl bromide, DMF, K<sub>2</sub>CO<sub>3</sub>, 80°C, 72 h. III) THF, NaOH (aq) 5%, 12 h.

Synthesis of dimethyl 2-aminoterephthalate (**3**)



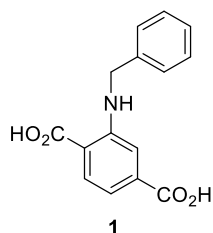
Aminoterephthalic acid **2** (0.187 g, 10.0 mmol), MeOH (4,5 mL), and concentrated H<sub>2</sub>SO<sub>4</sub> (390  $\mu$ L, 7.23 mmol) were added on an ACE<sup>®</sup> high pressure tube and then the tube was closed. The resulting mixture was kept under magnetic stirring at 70°C for 18 h. The reaction was then allowed to cool to room temperature, and it was neutralized by addition of saturated aqueous NaHCO<sub>3</sub> solution until pH 7 was reached. After extraction with EtOAc the combined organic layers were concentrated under vacuum and the crude product was purified by column chromatography over silica gel and a mixture of hexane and ethyl acetate 8:2 as eluent to give 144 mg of compound **3** (6.9 mmol, 69 %). <sup>1</sup>H-NMR (400 MHz, CDCl<sub>3</sub>)  $\delta$  7.91 (d, *J* = 8.6 Hz, 1H), 7.35 (d, *J* = 1.6 Hz, 1H), 7.26 (d, *J* = 1.6 Hz, 1H) 7.24 (d, *J* = 1.6 Hz, 1H) 5.82 (s, 2H), 3.91 (s, 3H), 3.89 (s, 3H); <sup>13</sup>C NMR (100 MHz, CDCl<sub>3</sub>)  $\delta$  168.1, 166.6, 150.1, 134.8, 131.5, 118,0, 113.9, 52.4, 51.9.

Synthesis of dimethyl 2-benzylaminoterephthalate ester (**4**)



To an ACE® pressure tube was added the compound **3** (71,5 mg, 0,342 mmol), dry DMF (3,0 mL), dry potassium carbonate (70,8 mg, 0,512 mmol) and then benzyl bromide (45,0  $\mu$ L, 0,379 mmol). The resulting mixture was kept under magnetic stirring at 80°C for 72 h. After the addition of water (50 mL), the reaction was extracted with ethyl acetate (3 x 50 mL) and the organic phase was joined and washed with distilled water (50 mL). The solvent was removed under reduced pressure and the crude product was purified by column chromatography over silica gel and a mixture of hexane and ethyl acetate 8: 2 as eluent affording 23.8 mg of compound **4** (0,0795 mmol, 23%). <sup>1</sup>H-NMR (400 MHz, CDCl<sub>3</sub>)  $\delta$  8.16 (s, 1H), 7.97 (dd, *J* = 8.3, 4.5 Hz, 1H), 7.39 – 7.34 (m, 5H), 7.26-7.31 (m, 1H), 7.22 (dd, *J* = 8.3, 1.6 Hz, 1H), 4.49 (d, *J* = 5.5 Hz, 2H), 3.87-3.89 (m, 6H). <sup>13</sup>C NMR (101 MHz, CDCl<sub>3</sub>)  $\delta$  168.6, 166.8, 150.6, 138.3, 135.2, 131.8, 128.8, 127.4, 127.3, 115.2, 113.3, 112.76, 52.3, 51.8, 47.1.

#### Synthesis of 2-benzylaminoterephthalic acid (**1**)



To an ACE® pressure tube was added the compound **4** (23.8 mg, 0.080 mmol), 1.0 mL of THF and 300  $\mu$ L of 4% KOH aqueous solution. The resulting mixture was kept overnight under magnetic stirring at 65°C. After this time, the reaction was neutralized using a 1.0 M HCl aqueous solution and then it was extracted with ethyl acetate (3 x 50 mL). The organic phase was washed with distilled water, dried with anhydrous sodium sulfate and filtered off. The solvent was removed under vacuum and the crude product was purified by recrystallization using ethyl acetate and hexane. The precipitate was collected by filtration, washed with hexane and then dried under vacuum furnishing compound **1** in 93% yield (20.0 mg, 0.074 mmol). <sup>1</sup>H NMR (400 MHz, DMSO)  $\delta$  8.32 (s, 1H), 7.90 (d, *J* = 8.2 Hz, 1H), 7.36 (d, *J* = 4.4 Hz, 4H), 7.31 – 7.24 (m, 1H), 7.22 (d, *J* = 1.4 Hz, 1H), 7.10 (dd, *J* = 8.2, 1.4 Hz, 1H), 4.51 (s, 2H). <sup>13</sup>C NMR (101 MHz, DMSO)  $\delta$  169.5, 167.0, 150.3, 134.0, 135.6, 131.9, 128.6, 127.0, 126.9, 114.8, 113.6, 112.3, 45.8.

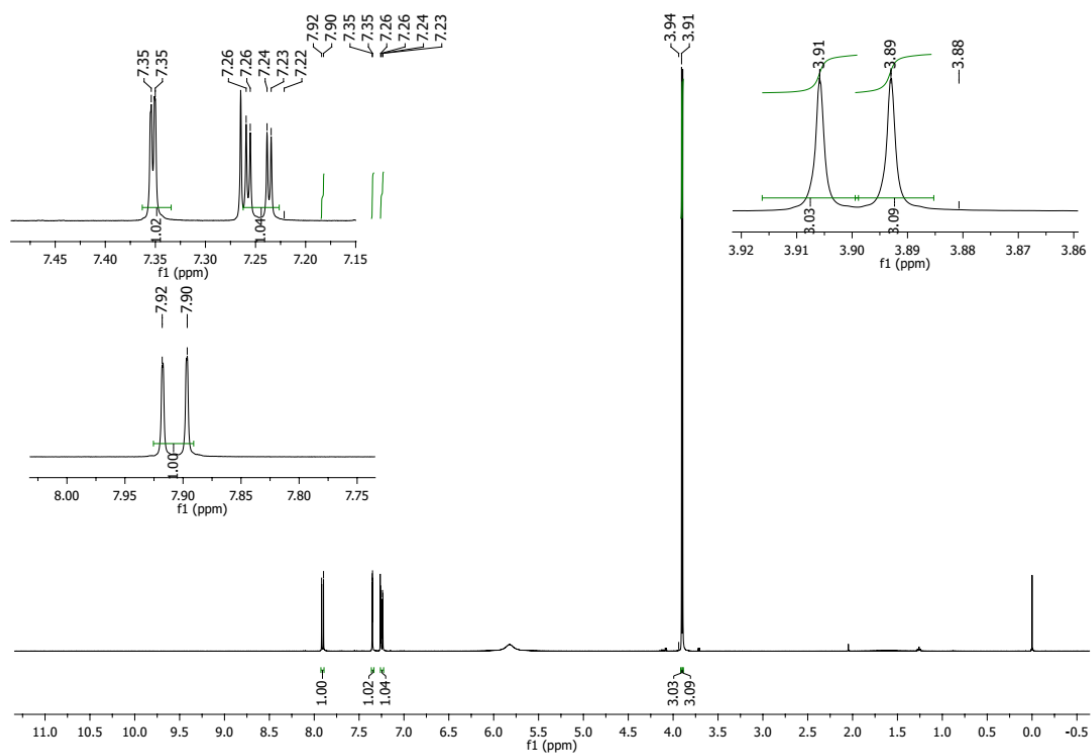


Figure S19:  $^1\text{H-NMR}$  spectra of dimethyl 2-aminoterephthalate (3) in  $\text{CDCl}_3$ .

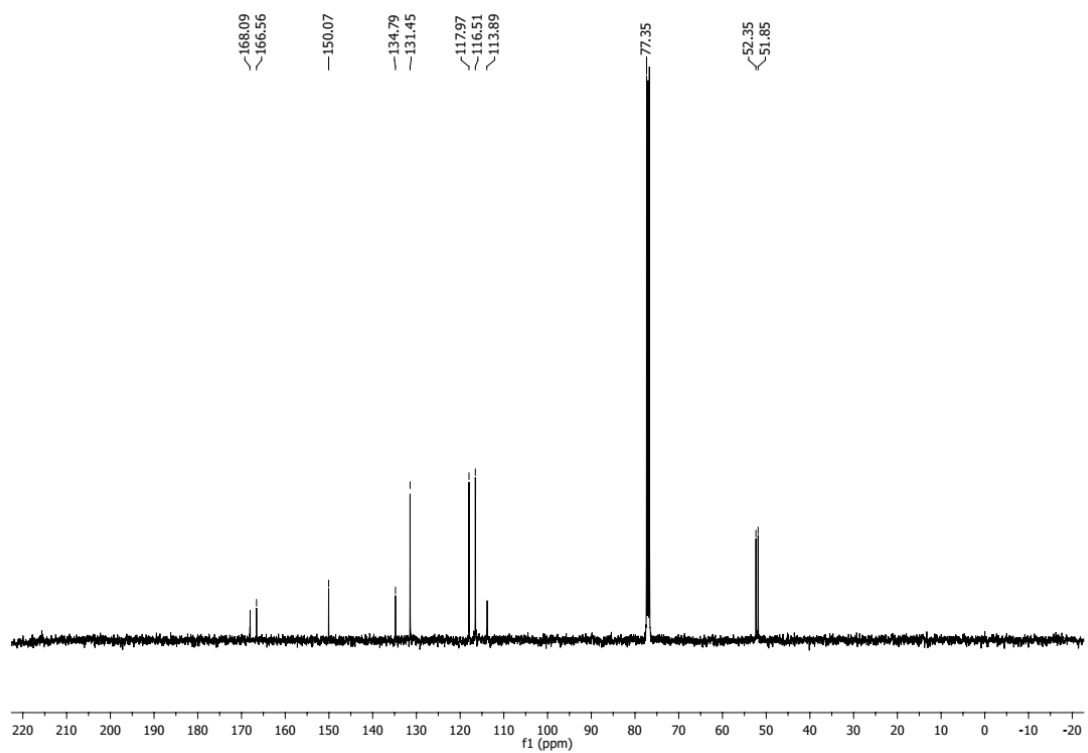


Figure S20:  $^{13}\text{C-NMR}$  spectra of dimethyl 2-aminoterephthalate (3) in  $\text{CDCl}_3$ .

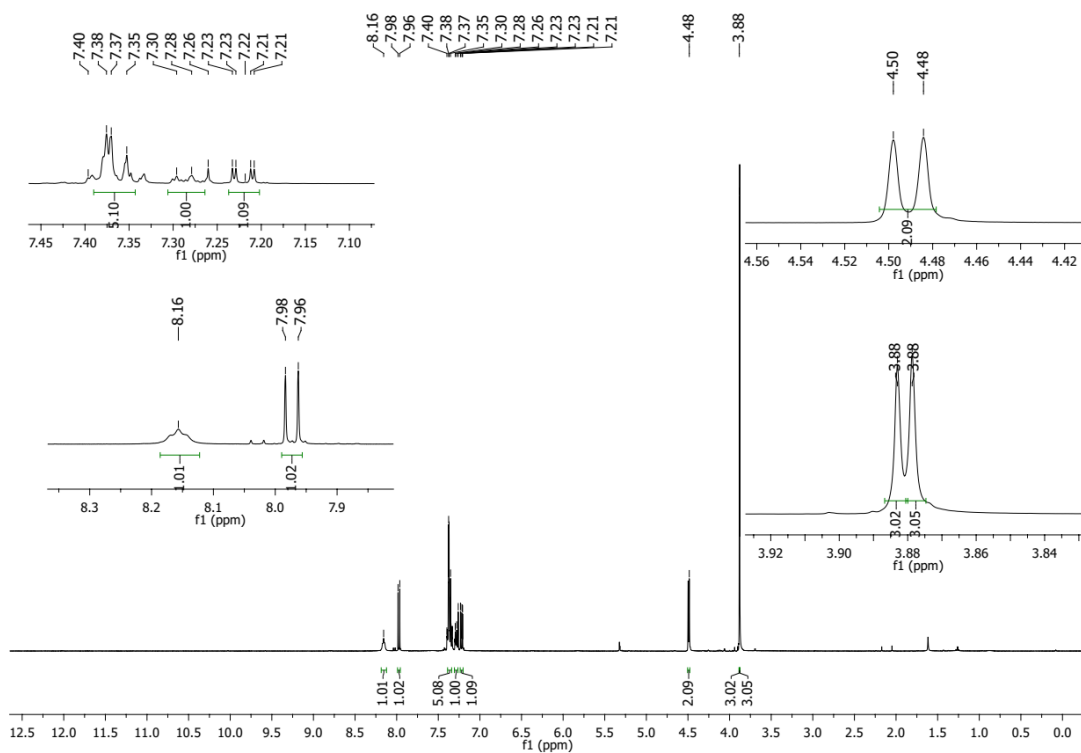


Figure S21:  $^1\text{H-NMR}$  spectra of dimethyl 2-benzylaminoterephthalate (4) in  $\text{CDCl}_3$ .

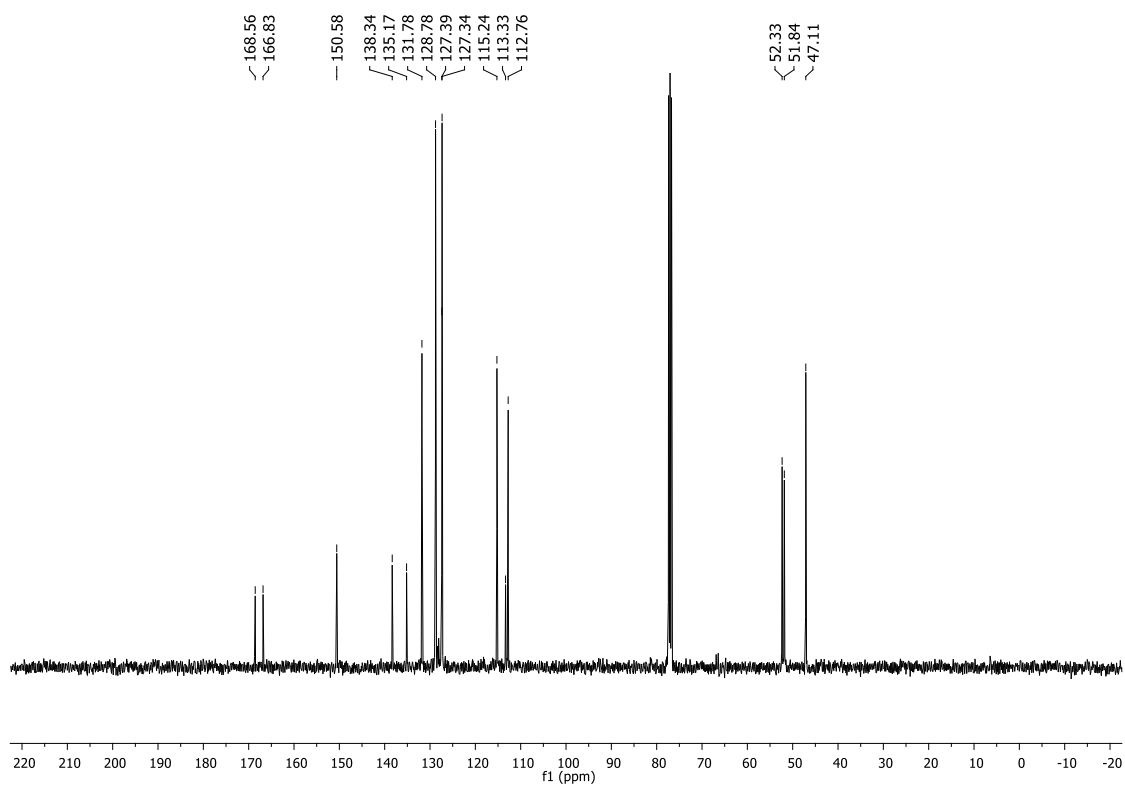


Figure S22:  $^{13}\text{C-NMR}$  spectra of dimethyl 2-benzylaminoterephthalate (4).



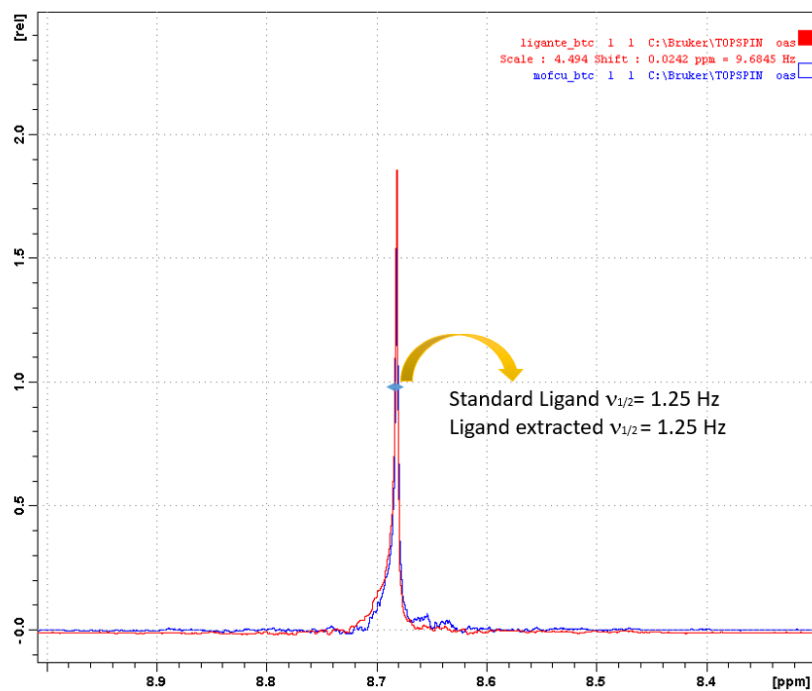
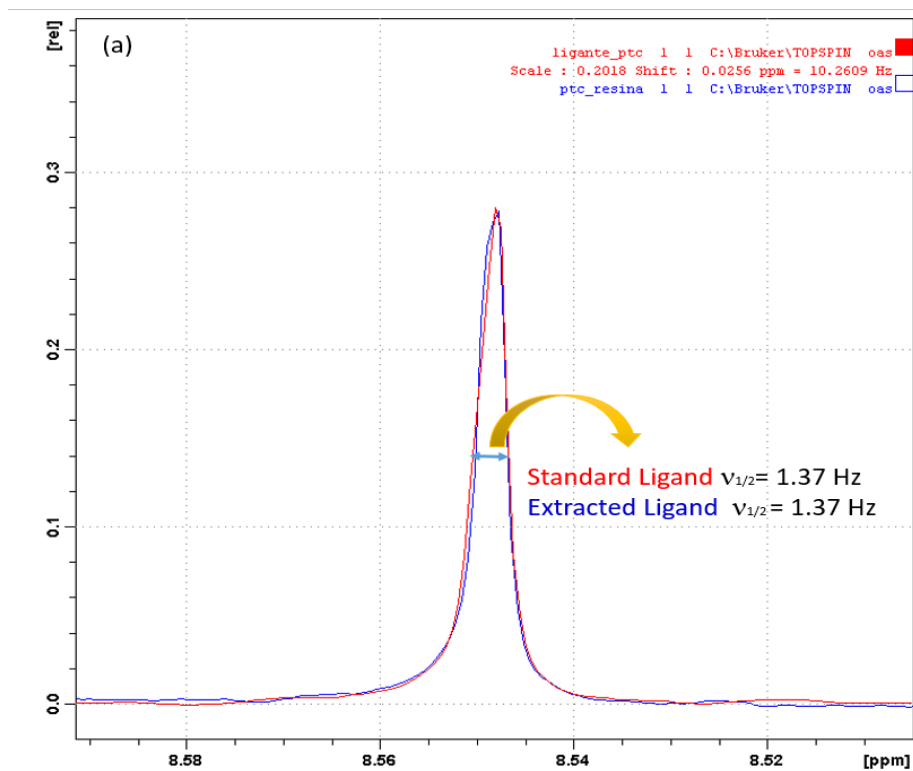


Figure S25: Comparative matching and bandwidth between the standard ligands and the ligand obtained from ion exchange treatment (a)  $[\text{Eu}_2(\text{H}_2\text{O})_5(\text{ptc})_2] \cdot \text{H}_2\text{O}$  and pyridine tricarboxylic acid (ptc), (b)  $\text{HKUST-1}[\text{Cu}_2(\text{btc})_3]$  and benzene tricarboxylic acid (btc).



### **S13 Scanning electron microscopy (SEM)**

SEM images of  $[\text{Eu}_2(\text{H}_2\text{O})_5(\text{ptc})_2] \cdot \text{H}_2\text{O}$  and  $[\text{Gd}_2(\text{ofd})_3 \cdot 8\text{H}_2\text{O}]$ , shown in Figures S26 and S27, respectively, confirm the highly anisotropic morphology of the materials: plate-like crystals and needle-like crystals, respectively. This corroborates that the powder XRD patterns of these two materials are particularly affected by preferred orientation.

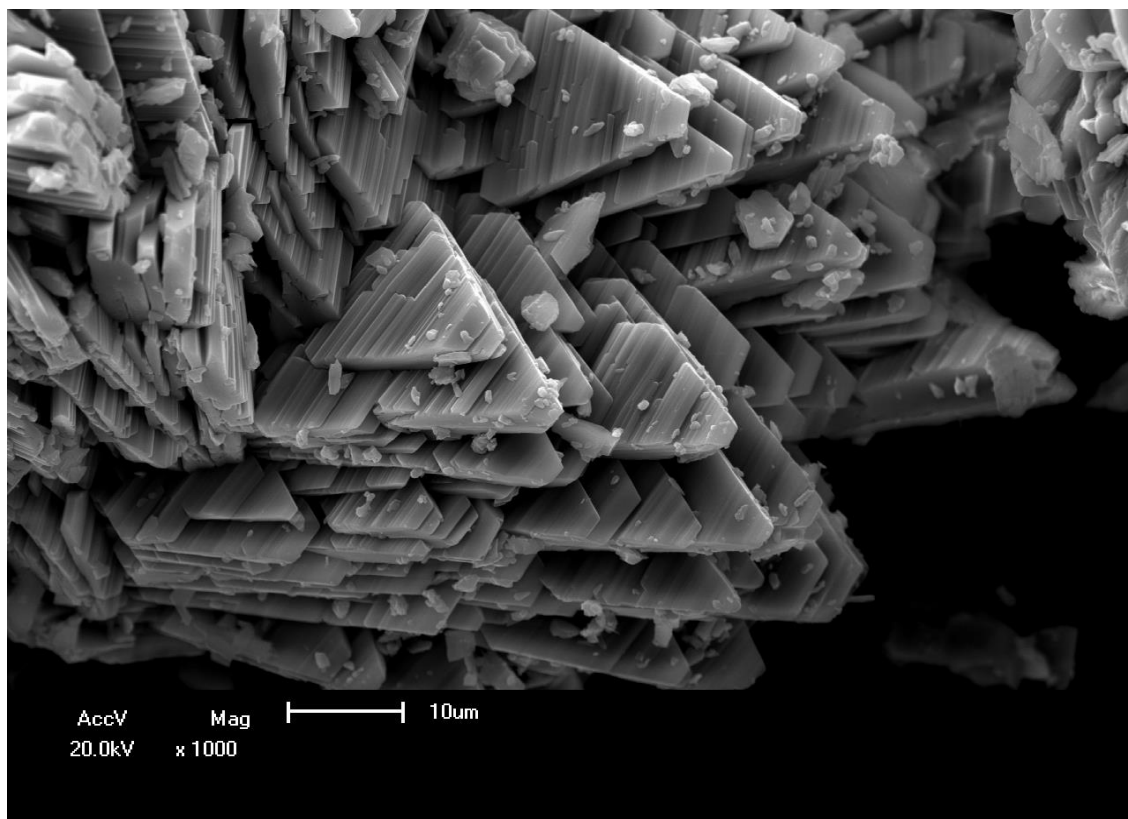


Figure S26: SEM image of  $[\text{Eu}_2(\text{H}_2\text{O})_5(\text{ptc})_2] \cdot \text{H}_2\text{O}$

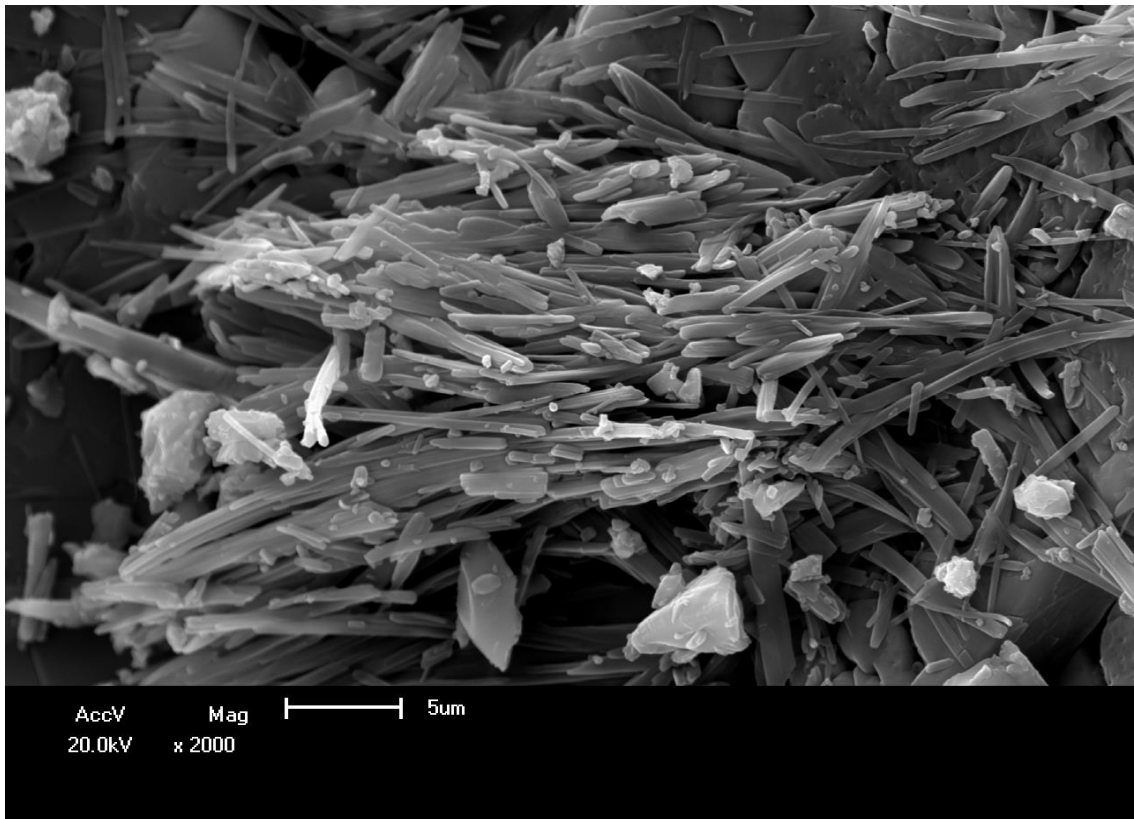


Figure 27: SEM image of  $[\text{Gd}_2(\text{ofd})_3 \cdot 8\text{H}_2\text{O}]$

## References

1. S. S.-Y. Chui, S. M.-F. Lo, J. P. H. Charmant, A. G. Orpen and I. D. Williams, *Science*, 1999, 283, 1148–1150.
2. W. Hongsheng, Z. Xiaoqing, L. Mingli, S. Wei and C. Peng, *Chin. J. Chem.*, 30, 2097-102.
3. Y. Jiang, X-S. Wu, X. Li, J-H. Song and Y-Q. Zou, *J. Coord. Chem.*, 2010, 63, 36-45.
4. M. Eddaoudi, J. Kim, N. Rosi, D. Vodak, J. O’Keefe. Wachter, O. M. Yaghi, *Science.*, 2002, 295, 469-472.
5. E. Dugan, Z. Wang, M. Okamura, A. Medina, S. M. Cohen, *Chem.Commun.*, 2008, 3366-3368
6. F. Millange, N.Guillou, M.E. Medina, G. Férey, A. Carlin-Sinclair, K.M. Golden and R.I. Walton, *Chem. Mater.* **22**, 2010, 4237–4245.
7. You-Kyong Seo, Geeta Hundal, In Tae Jang, Young Kyu Hwang, Chul-Ho Jun, Jong-San Chang, *Micropor. Mesopor. Mater.* **119** (2009) 331–337.
8. J-Li Lin, W. Xu, L. Zhao and Y.-Qing Zheng, *Z. Naturforsch.* **66b**, 2011, 570 – 576.
9. Z. Wang and S.M. Cohen, *Angew. Chem., Int. Ed.* **47**, 2008, 4699-4702
10. A.Ranft, S.B. Betzler, F. Haase and B.V. Lotsch, *CrystEngComm* **15**, 2013, 9296
11. J. Liu, X. Zhang, J. Yang and L. Wang, *Appl. Organometal. Chem.* **28**, 2014, 198–203